- 1 MICROSTRUCTURAL CHARACTERISTICS OF BIOSOURCED CONCRETES
- 2 REINFORCED WITH SUGAR CANE BAGASSE FIBERS: CASE OF ETTRINGITE
- 3 FORMATION AND C-S-H PROPAGATION

Abstract: In this work, we studied ettringite formation, C-S-H propagation, and the thermomechanical properties of sugarcane bagasse (SBC) fiber-reinforced concrete with a maximum dosage of 0.17% by weight. Scanning electron microscopy (SEM), thermogravimetric analysis (TGA), and infrared (IR) analyses were performed. TGA results showed biobased concrete resistant to temperatures exceeding 500°C. TGA results revealed thermal stability of bio-based concrete. SEM analysis showed ettringite and C-S-H propagation without altering mechanical properties. These results are consistent with those obtained by other authors.

11 Keywords: Concrete, bagasse fiber, thermogravimetric analysis, ettringite, C-S-H, SEM.

1.Introduction

Replacing traditional building materials with bio-based alternatives with low thermal conductivity (or high thermal resistance) has become an attractive solution for improving the thermal efficiency and reducing the carbon footprint of buildings [1][2]. Bio-based materials possess hygroscopic properties that make them effective as thermal insulators and contribute to a healthier and more comfortable living environment. It is in this sense that the development of bio-based concrete occupies an important place [1][3]. Plant-based products offer an ecological and renewable option due to their sustainability criteria, such as local availability and low processing costs. The thermal resistance of conventional mortars was improved by 16% and 36% with the addition of 10% and 20% cork [4]. When concrete is subjected to an increase in temperature, various physical and chemical transformations occur [5]. Sugarcane bagasse, incorporated into the concrete matrix, reacts with the free CH present in the concrete to form the C-S-H network, strengthening the strength of the concrete [6]. Thermogravimetric analysis (TGA) is a widely used technique for the study of materials. It allows the determination of different hydrates and carbonates. TGA allows understanding material-specific reactions such as dihydroxylation, decarbonization, decomposition or changes in the crystalline structure [7]. Our work aims to study the microstructural characteristics of bio-sourced concretes from sugarcane bagasse fibers using TGA, SEM and IR on all concretes.

2. Materials and Methods

We used the materials and methods described in our previous article [8].

3. Characterization Methods

3.1. Microstructural Observations by Scanning Electron Microscopy (SEM)

Microstructure was observed by scanning electron microscopy (SEM) on fresh concrete fragments from cylindrical samples after 28 days of storage. The instrument used was a Hitachi TM3030Plus with a beam accelerating voltage of 20 keV and a probe current of 150 to 250 pA. Before being subjected to the SEM, the samples were metallized with gold after drying at 40°C. The microstructures observed by SEM of the biofiber-reinforced concrete (SBC-15), polypropylene concrete (PC), and reference concrete (OC) are presented in Figures 1, 2, 3, and 5 below.

3.2. Thermogravimetric Analysis (TGA)

The analysis was performed on powdered concrete fragments obtained by grinding to a thickness of less than 315 mm, from cylindrical samples after 28 days of storage. The instrument used was the NETZSCH Tarsus TG209F3 model. Measurements began at an initial temperature of 30°C and ended at 600°C, with a heating rate of 10°K/min. The NETZSCH pellets (25 μ L) used are made of aluminum and can withstand a maximum temperature of 600°C.

3.3. Infrared Spectrometry (IR)

This is an analytical technique used to determine the chemical composition and structure of materials. The analysis was performed on fresh concrete fragments from cylindrical samples after 28 days of storage. The instrument used was the Spectrum Two FT-IR Spectrometer. Analyses were performed on residues from the ATG.

4. Results and Discussion

4.1. Microstructural Observations by Scanning Electron Microscopy (SEM)

4.1.1. Ordinary Concrete (OC)

Figure 1 shows the microstructures of the OC samples. Concrete hydrates such as ettringite needles and hydrated calcium silicate (C-S-H) can be observed.

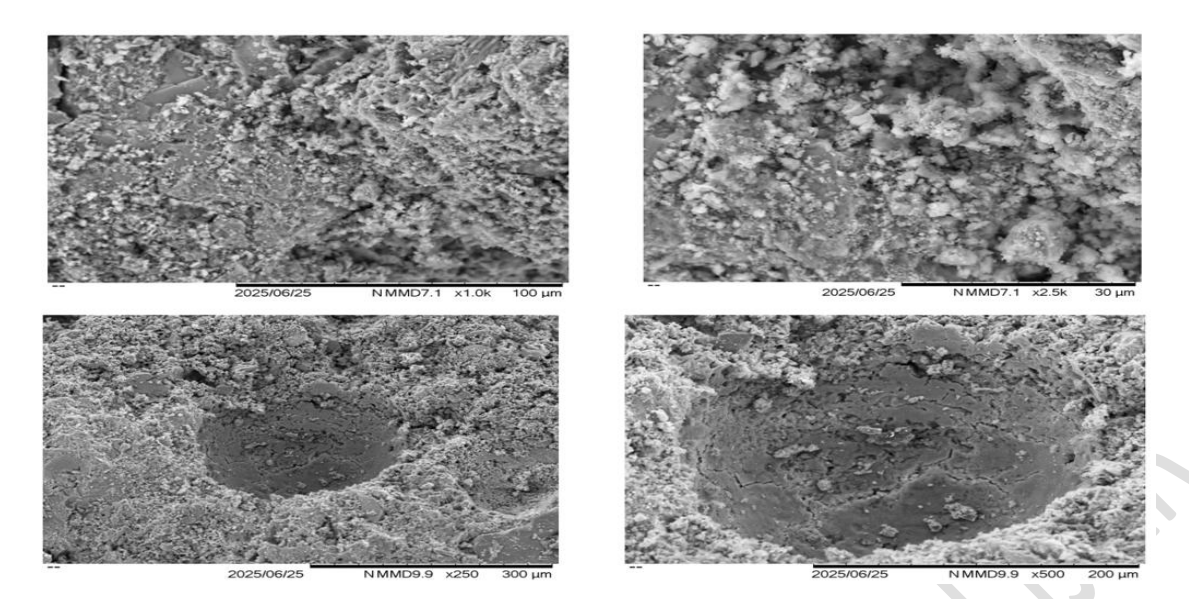
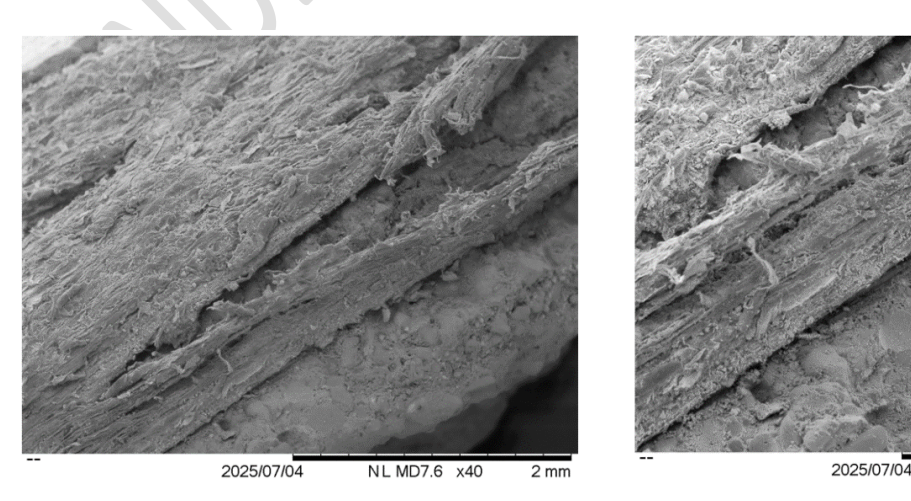


Figure 1: SEM of OC concrete

Secondary ettringite formation is closely related to the transport of pore fluids within the concrete mass. The deterioration of a large number of concrete structures in contact with sulfate-free environments and related to secondary ettringite formation is currently one of the major research problems, very controversial for researchers.sustainable materials [9]. Research on this topic suggests that the explanation for this phenomenon lies in the rapid absorption of sulfates by calcium silicate hydrate (C-S-H), thus preventing the usual formation of ettringite at an early stage. Later, the release of these sulfates into the pore fluid of the concrete causes the crystallization of ettringite. Expansion phenomena, existing cracks, and diffusion processes within the material play a key role throughout this process [10]. Sulfate can be combined by the C-S-H gel at an early stage of hydration and released at a later stage. The sulfate required for secondary ettringite formation comes from hydrated Portland cement. Concrete deterioration due to delayed ettringite formation can be attributed to an increase in temperature during concrete curing [10].

4.1.2. Sugarcane bagasse fiber concrete (SBC-0.15) not subjected to thermal stress

Figure 2 below shows the SEM of bagasse fiber concrete made with SBC-0.15.



SEM images of

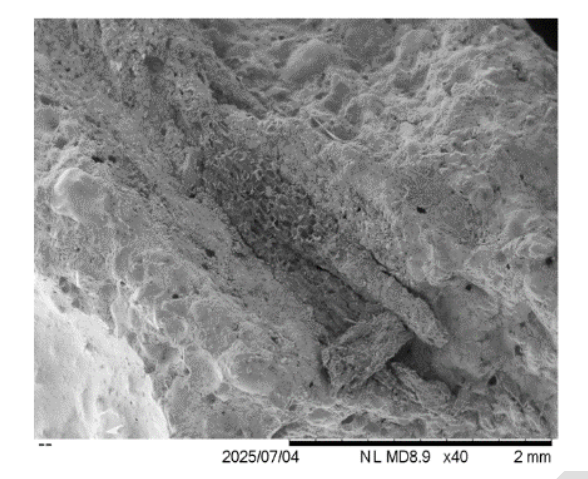
Figure 2: SEM of SBC-0.15

77 SBC-0.15 confirm the

porous structure and water absorption capacities of the fiber. This allows good adhesion with the concrete matrix. Ettringite and hydrates appear less compared to polypropylene fiber concrete. This justifies good porosity of the fiber. Bagasse fiber does not trap air as is the case with polypropylene fiber which has better porosity. Many cavities can be observed, probably due to the evaporation of water absorbed by the fibers during the pre-soaking phase or related to air trapped during mixing [11][12].

4.1.3. Sugarcane bagasse fiber concrete (SBC-0.15) subjected to thermal stress

Figure 3 below shows the SEM of SBC-0.15 subjected to thermal stress



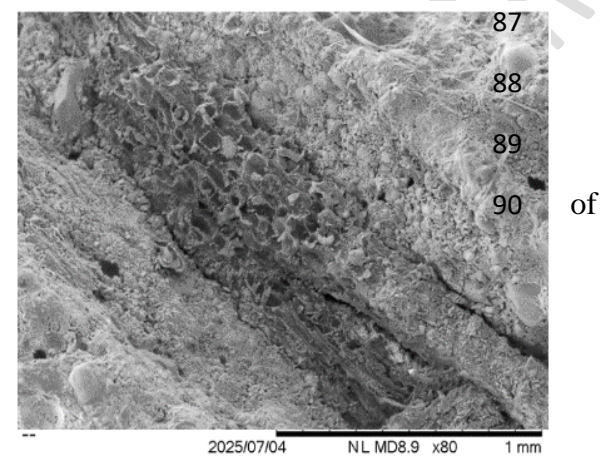


Figure 3: SEM of SBC-0.15 subjected to thermal stress

1000°C in a CERADEL C86 –160 C2 electric kiln. A heating phase at a speed of 1°C/min up to

the predefined temperature T°C. The kiln can reach a temperature of 1300°C, the temperature is predefined in advance during a technical adjustment of the device. A fan associated with the heating allows the temperature to be regulated and homogenized by the circulation of air between the heating resistors. Figure 4 below shows the electric furnace containing the concretes.





Figure 4: Electric furnace containing the concrete

The bagasse fiber was able to resist in this aggressive environment [13]. We can observe the porous network of the bagasse fiber and an expansion of the concrete matrix due to thermal stress. In Figure 4, the microcracks can be explained by the expansion of the sugarcane bagasse fiber during melting, which generates stresses and consequently the formation of

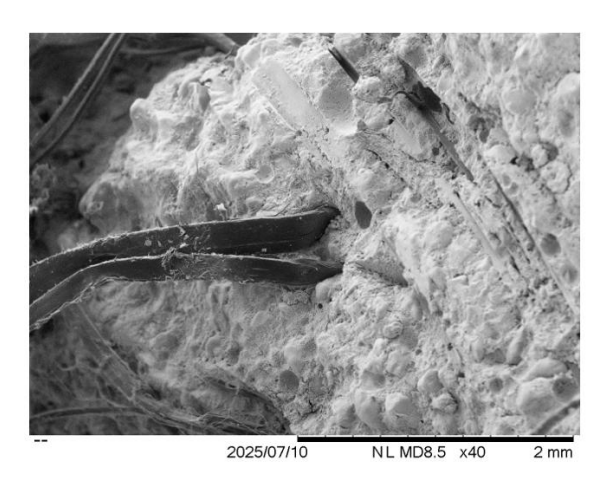
cracks. The presence of the fibers modifies the geometry and morphology of the network

Porous. This phenomenon is due to the loss of water initially contained in the C-S-H hydrates

112 [14][15].

4.1.4. Polypropylene (PC) fiber concrete

Figure 5 shows the SEM of concrete made with polypropylene fibers.



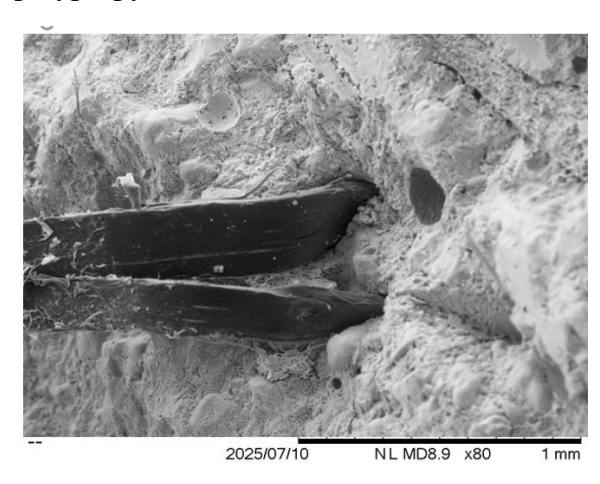


Figure 5 : SEM of PC at room temperature

Calcium-silica-hydrate (C-S-H) gels and ettringite generally appear in lighter shades. Hydrates and ettringites are found to cover all concrete fibers and layers, acting as a binder, which can lead to pore-blocking, reduced permeability, and reduced porosity. Polypropylene fibers can also be said to trap air in the mix, increasing void volume and not improving porosity. As a consequence, this can lead to a decrease in compressive strength [16] [17].

4.2. Concrete Thermal Stability Measurements: Thermogravimetric Analysis (TGA)

The analysis was conducted on powdered concrete fragments obtained by grinding to a thickness less than 315 mm, from cylindrical samples after 28 days of storage. The device used is the NETZSCH Tarsus TG209F3 model. Measurements begin at an initial temperature of 30°C and end at a temperature of 600°C, with a heating rate of 10° K/min. The NETZSCH pellets (25 μ L) used are made of aluminum and can withstand a maximum temperature of 600°C.

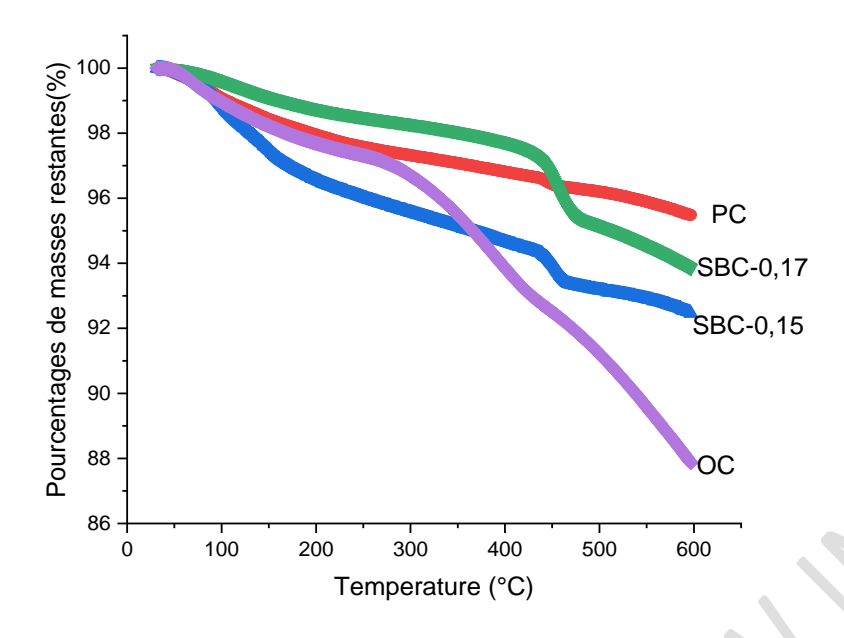


Figure 6: ATG curves of the different selected concretes

Figure 6 shows typical mass loss curves during a temperature increase of 10° C/min. The first derivative signals (DTG) for the different concretes are given in Figures 7, 8 and 9

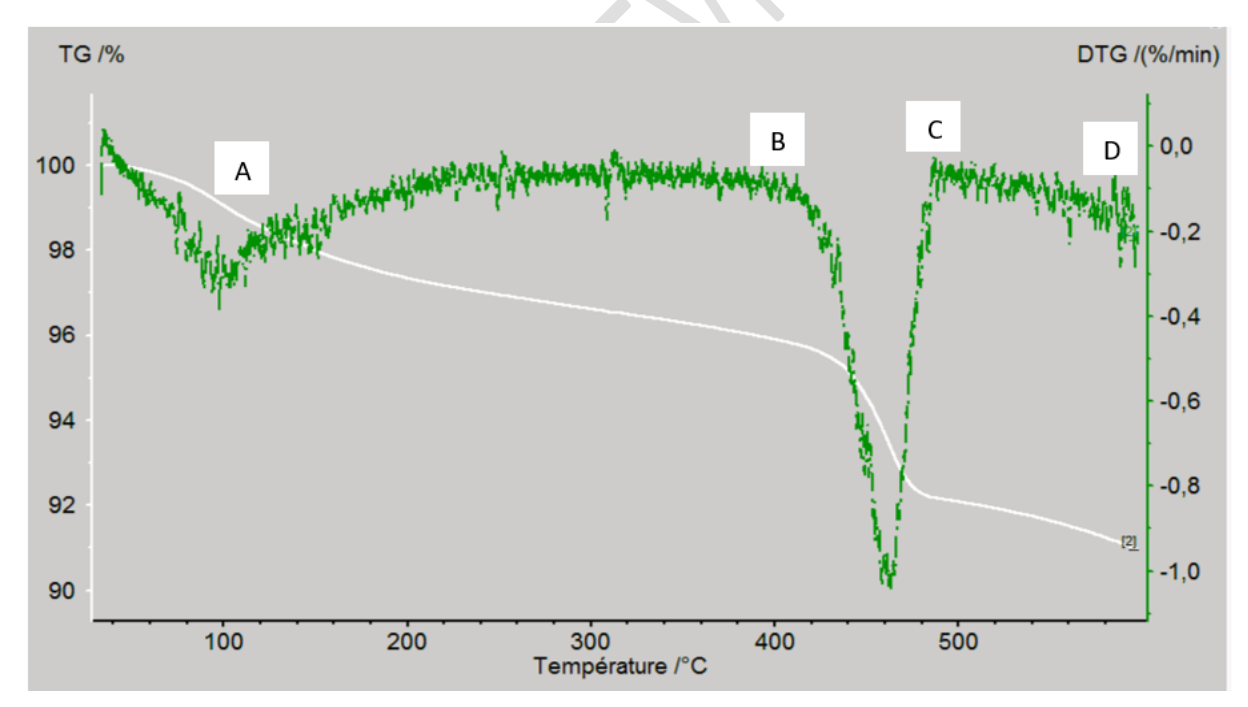


Figure 7: DTG curve of OC concrete. The recorded curve for the ATG of OC is superimposed for comparison purposes (in white).

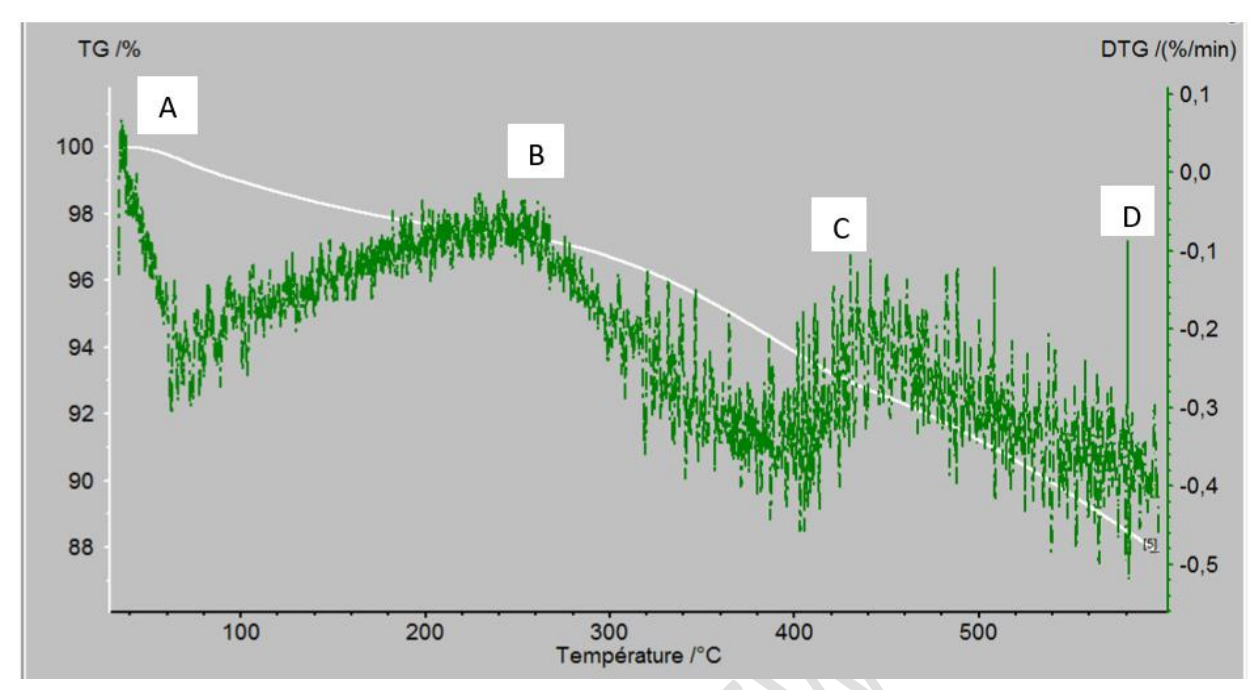


Figure 8: DTG curve of SBC-15 concrete. The recorded curve for the ATG of SBC-15 is superimposed for comparison (in white)

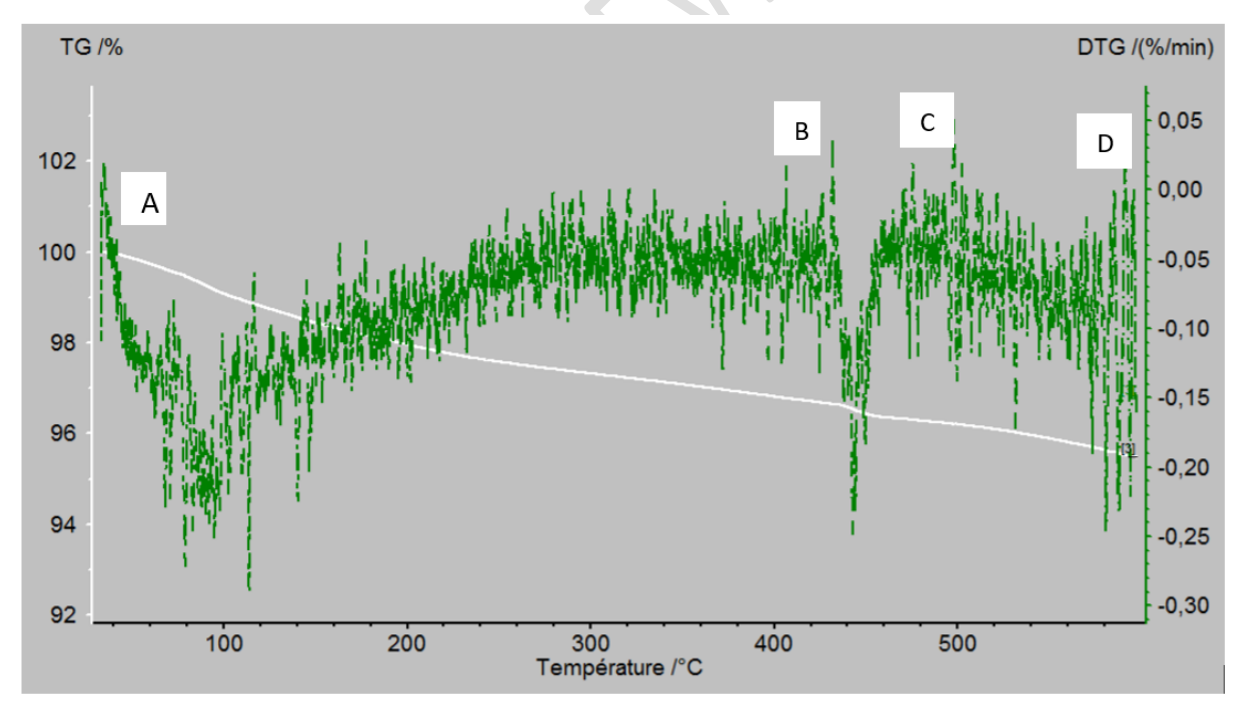


Figure 9: DTG curve of PC concrete. The recorded curve for the ATG of PC is superimposed for comparison purposes (in white)

Several degradation phases are observable on these curves, closely related to the composition of the concretes. Regarding ordinary concrete (OC), three distinct stages are observed, revealing the products generated by the hydration reactions between cements and water [18]. In Figure 7, the first sign of mass loss is perceptible between 35 and 135 °C, as indicated by

peak A on the DTG curve. This loss results from both the evaporation of capillary water and the elimination of water associated with ettringite hydrate. The mass loss observed between 400 and 500 °C can be attributed to the release of water present in hydrated calcium silicates (C-S-H), and to the dehydroxylation of portlandite (Ca(OH)2). Finally, the mass loss in the temperature range of 500 to 600 °C, i.e. between C and D, corresponds to the decarbonation of calcium carbonate; it is probably linked to poorly crystallized carbonate compounds [19].

Regarding the formulations of concretes containing sugarcane bagasse fibers, specific characteristics can be highlighted. In Figure 8, the TGA results indicate that the overall weight loss observed between 400 and 500 °C is significantly higher than that of OC concrete and that this difference increases as the fiber content increases. This can be attributed to the evaporation of excess water used to pre-soak the fibers and preserve the workability of the concretes, as well as to the degradation of bagasse fibers under the effect of the kiln heat. The degradation trends of bio-based concretes, as illustrated by the DTG curve of SBC-0.15 (Figure 8), are similar to those previously observed for OC concrete. This indicates the presence of the same cement hydrates, such as ettringite, portlandite and calcium carbonate hydrates. A notable difference is the slowing of the peak at points C and D, indicating a higher relative proportion of calcium carbonate.

This deduction can be attributed to the higher porosity, demonstrated by SEM analysis, which makes these bio-based concretes more sensitive to carbonation. The amplitude of the DTG peak at point A in bio-based concretes is significantly higher than that of ordinary OC concrete. This can be explained due to the evaporation of residual water from sugarcane bagasse fibers. The amplitude of the DTG peak at points B and C related to portlandite is broader, compared to that in Figure 6 of ordinary concrete. This is explained by the incorporation of sugarcane bagasse fibers. This result suggests that the sugar molecules extracted from sugarcane bagasse fibers had no negative impact on cement hydration. Alkalipretreated sugarcane bagasse fibers contain low hemicellulose content compared to untreated fibers [20].

Regarding the ATG of PC concrete, the lack of porosity of the polypropylene fibers explains why the PC curve has the best result out of all the curves in Figure 6. In Figure 9, we observe a first weight loss at peak A, which is due to the evaporation of water from the capillary voids, which represent the space not occupied by the hydrated cement during the hydration process. Between 100 and 200°C, the polypropylene fibers melt very quickly, causing channeling, thus releasing heat pressure in the concrete. Observing Figure 9, between 200 and 500°C, that is, between point A and point C, the weight loss continues due to the loss of water in the concrete, as well as the subsequent decomposition of the polypropylene fibers. Between points B and C, the loss rate dropped sharply. This increase is due to the decomposition of calcium hydroxide in the cement paste as well as the decomposition of the C–S–H phase of ettringite, followed by the formation of beta-dicalcium silicate (b–C2S) [21].

4.3. Infrared Spectrometry (IR)

Figure 10 below shows the IR transmission spectra of the different concretes analyzed after TGA.

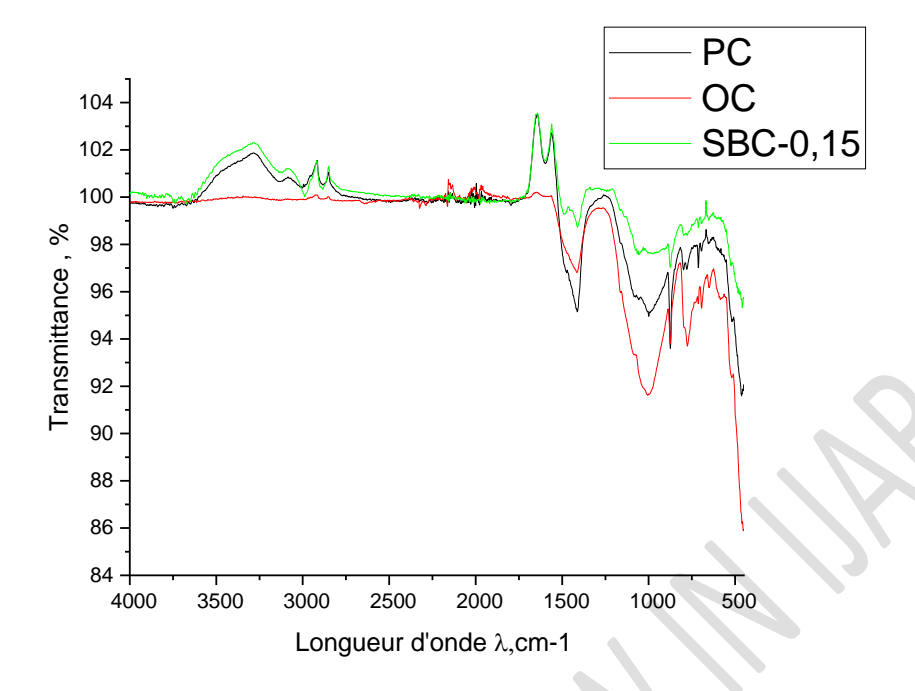


Figure 10: IR curves of different concretes

The results of SBC-0.15 bio-fibered concrete show different peaks between 2000 cm-1 and 1500 cm-1. This peak is associated with the O-H stretching vibration observed in cellulose, hemicelluloses and lignin which are the main sugar compounds [22]. The peaks in the SBC-0.15 curve are attributed to the asymmetric and symmetric C-H stretching vibrations of CH2 in cellulose and hemicelluloses, respectively. Further, we can add that the two peaks are attributed to the O-H bending vibrations of water absorbed by cellulose and the C=O stretching of carboxylic acid and ester, respectively [23]. The IR spectroscopy results confirm the SEM images and TGA curves of bio-fibered concretes. They show that sugarcane bagasse fiber contains high concentrations of C, H, and O. These elements are combined into different functional groups characterized by different stretched wavenumbers, such as hydroxyl (O-H), hydrocarbon (C-H), and carbonyl (C-O) groups.

5. Conclusion

In this study, we performed a microstructural characterization of sugarcane bagasse fiber-reinforced concretes. We performed SEM, TGA, and IR on all concretes. The results of thermogravimetric analyses at 600°C of the bio-based bagasse fiber concretes are very similar to those of the polypropylene fiber concrete. SEM observations of the bio-based concretes show the propagation of ettringite and C-S-H. This propagation does not affect the thermomechanical strength of the concretes. In all SEM observations, the bagasse fiber is integrated into the concrete matrix, which appears to provide a satisfactory environment for the formation of ettringite and the release of C-S-H. The porous nature of the sugarcane bagasse fiber prevents the propagation of air bubbles, which is not the case for the polypropylene fiber. This is not the case for polypropylene fiber. The IR results of bio-based concrete confirm the TGA findings. Additional experimental evidence is needed to study the propagation of ettringite and C-S-H. Sudden cooling of the concrete matrix can create

- 213 favorable conditions for matrix deterioration and ettringite formation. Sugarcane bagasse fiber
- 214 has very good incorporation qualities in concrete. It can therefore replace polypropylene fiber.
- 215 It withstands high temperatures without significantly altering its mechanical properties. This
- 216 study once again confirms its status as an ecological material for green, sustainable, and
- optimizable construction, as advocated by the United Nations.

218 Acknowledgments

- The authors thank the University of Reims Champagne-Ardenne (France) and the Congo
- National Petroleum Company Foundation (SNPC) for their contribution to this work.

221 Conflict of Interest

The authors declare no conflict of interest regarding the publication of this article.

223 References

- 224 [1] Amziane, S. and Mohammed, S., (2016), "Overview on biobased building material made
- 225 with plant aggregate", RILEM Technical Letters, vol. 1, pp.31-38.
- 226 <u>https://doi.org/10.21809/rilemtechlett.2016.9</u>
- 227 [2] Chel, A. and Kaushik, G., (2018), "Renewable energy technologies for sustainable
- development of energy efficient building", Alexandria Engineering Journal, vol.57, pp.655-
- 229 669. https://doi.org/10.1016/j.aej.2017.02.027.
- 230 [3] Amziane, S. and Collet, F., (2017), "Bio-aggregates based building materials state-of-
- the-art report of the RILEM technical committee 236-BBM", Springer Netherlands, 203
- pages. https://doi.org/10.1007/978-94-024-1031-0
- 233 [4] Panesar, D. and Shindman, B., (2012), "The mechanical, transport and thermal properties
- of mortar and concrete containing waste cork", Cement and Concrete Composites, vol.34,
- pp.982-992. https://doi.org/10.1016/j.cemconcomp.2012.06.003.
- 236 [5] Noumowé, A., (1995), "Effet Des Hautes Températures (20-600°C) Sur Le Béton : Cas
- Particulier Du Béton à Hautes Performances ", Thèse de doctorat, Institut National des
- 238 Sciences Appliquées de Lyon, 196 pages.
- 239 [6] Indukuri, S.S.R., Nerella, R. and Madduru S.R.C., (2019), "Effect of graphene oxide on
- 240 microstructure and strengthened properties of fly ash and silica fume based cement
- composites", Construction and Building Materials, vol. 229, ID:116863,
- 242 https://doi.org/10.1016/j.conbuildmat.2019.116863
- Hohne, G.W.H., Hemminger, W.F., and Flammersheim, H. J., (2003), "Differential
- Scanning Calorimetry", Berlin Heidelberg: Springer, 298 pages.
- 245 [8] Malanda Ceti, C.A., Dzabana Honguelet, A.S., Ngoro-Elenga, F., Nsongo, T.,
- Eboungabeka, A.D., Elenga, H. and Mfoutou, N.N., (2024), "Influence of Sugarcane Bagasse
- Fibers on the Mechanical Strength and Porosity of Concrete Made with Forspak 42.5 N

- 248 Cement in the Republic of Congo", Advances in Materials Physics and Chemistry, vol. 14,
- 249 249-263,
- 250 https://doi.org/10.4236/ampc.2024.1411018
- 251 [9] Batic, O.R., Milanesi, C.A., Maiza, P.J. and Marfil S.A., (2000), "Secondary ettringite
- 252 formation in concrete subjected to different curing conditions", Cement and Concrete
- 253 Research, vol. 30, pp. 1407 -1412, https://doi.org/10.1016/S0008-8846(00)00343-4
- 254 [10] Fu, Y., Xie, P., Gu, P. and Beaudoin, J.J., (1994), Significance of pre existing cracks on
- 255 nucleation of secondary ettringite in steam cured cement paste", Cement and Concrete
- 256 Researcher, vol. 24, pp. 1015-1024, https://doi.org/10.1016/0008-8846(94)90024-8
- 257 [11] Kirker A., Debicki, G., Bali, A., Khenfer, M.M. and Chabannet, M., (2005),
- 258 "Mechanical properties of date palm fibres and concrete reinforced with date palm fibers in
- 259 hot-dry climate", Cement & Concrete Composites, vol. 27, pp. 554–564,
- 260 <u>https://doi.org/10.1016/j.cemconcomp.2004.09.015</u>.
- 261 [12] Onofre Bustamante, E., et al., Cecilia Espindola-flores, C., A. and Cardenas de la
- Fuente, A.K., (2023), "study of integration, distribution and degradation of sugarcane bagasse
- 263 fiber as partial replacement for fine aggregate in concrete samples", cellulose chemistry and
- technology, Vol. 57, pp. 1121-1132. https://doi.10.35812/CelluloseChemTechnol.2023.57.98
- 265 [13] Zhutovsky, S. and Douglas Hooton, R., (2017), "Accelerated testing of cementitious
- 266 materials for resistance to physical sulfate attack", Construction and Building Materials, vol.
- 267 145, pp. 98–106, https://doi.org/10.1016/j.conbuildmat.2017.03.203.
- 268 [14] Noumowé, A., (2005), "Mechanical Properties and Microstructure of High Strength
- 269 Concrete Containing Polypropylene Fibers Exposed to Temperatures up to 200°C", Cement
- and Concrete Research, Vol. 35, pp. 2192–2198,
- 271 https://doi.org/10.1016/j.cemconres.2005.03.007
- 272 [15] Ozawa, M., Kim, G., Yoon, M., Sato, R. and Rokugo, K., (2017), « Thermal properties
- of jute fiber concrete at high temperature », Journal of Structure Fire Engineering, vol.7,
- pp.182–192, https://doi.org/10.1108/jsfe-09-2016-017. http://dx.doi.org/10.1108/JSFE-09-2016-
- 275 <u>017</u>
- 276 [16] Buyukozturk, O., Buehler, M., Lau D. and Tuakta C., (2011), "Structural solution using
- 277 molecular dynamics: Fundamentals and a case study of epoxy-silica interface", International
- Journal of Solids and Structures, vol. 48, pp. 2131-2140,
- 279 https://doi.org/10.1016/j.ijsolstr.2011.03.018
- 280 [17] Ramezanianpour A., Esmaeili, M., Ghahari, S.A. and Najafi, M.H., (2013), "Laboratory
- study on the effect of polypropylene fiber on durability, and physical and mechanical

- 282 characteristic of concrete for application in sleepers", Construction and Building Materials,
- vol. 44, pp.411-418,http://dx.doi.org/10.1016/j.conbuildmat.2013.02.076
- 284 [18] Eddhahak-Ouni A., Drissi, S., Colin, J., Neji, J. and Care, S., (2014), "Experimental and
- 285 multi-scale analysis of the thermal properties of Portland cement concretes embedded with
- microencapsulated Phase Change Materials (PCMs)", Applied Thermal Engineering, Vol. 64,
- 287 pp.32-39,
- 288 <u>https://doi.org/10.1016/j.applthermaleng.2013.11.050</u>
- 289 [19] Vogler N., Drabetzki, P., Lindemann, M. and Kuhne, H.C. (2022), "Description
- of the concrete carbonation process with adjusted depth-resolved thermogravimetric
- analysis", Journal of Thermal Analysis Calorimetry, vol. 147, pp. 6167-6180,
- 292 https://doi.org/10.1007/s10973-021-10966-1
- 293 [20] Boix E., Gineau, E., Onate Narciso, J., Hofte, H., Mouille, G. and Navard, P., (2020),
- "Influence of chemical treatments of miscanthus stem fragments on polysaccharide release in
- the presence of cement and on the mechanical properties of bio-based concrete materials".
- 296 Cement and Concret Composites, vol.105, ID:103429.
- 297 https://doi.org/10.1016/j.cemconcomp.2019.103429.
- 298 [21] Harmathy T.Z. and ALLEN L.W., (1973), "Thermal properties of selected masonry unit
- concretes", Journal of the American Concrete Institute, vol. 70, pp. 132–142,
- 300 https://doi.org/10.4224/40001663
- 301 [22] Bezazi A., Boumediri H., Garcia del Pino, G., Bezzazi B., Scarpa, F., Reise P. and
- DufresnefA., (2020), "Alkali Treatment Effect on Physicochemical and Tensile Properties of
- Date Palm Rachis Fibers", Journal of Natural Fibers, pp. 1–18,
- 304 https://doi.org/10.1080/15440478.2020.1848726.
- 305 [23] Dhegihan, A., Madadi Ardekani, S., Al-Maadeed, M., Hassan, A. and Uzir Wahit,
- 306 M.,(2013), "Mechanical and thermal properties of date palm leaf fiber reinforced recycled
- poly (ethylene terephthalate) composites", materials and design, vol. 52, pp. 841–848,
- 308 https://doi.org/10.1016/j.matdes.2013.06.022

314

